npg

ORIGINAL ARTICLE

A novel role of hematopoietic CCL5 in promoting triple-negative mammary tumor progression by regulating generation of myeloid-derived suppressor cells

Yan Zhang[1], Dandan Lv[2], Ha-Jeong Kim[1], Robert A Kurt[3], Wen Bu[4], Yi Li[4], Xiaojing Ma[1, 2, 5, 6]

[1]Department of Microbiology and Immunology, Weill Cornell Medical College, 1300 York Avenue, New York, NY 10065, USA; [2]School of Life Science and Biotechnology, Shanghai Jiao Tong University, Shanghai 200240, China; [3]Department of Biology, Lafayette College, Easton, PA 18042, USA; [4]Lester and Sue Smith Breast Center & Department of Molecular and Cell Biology, Baylor College of Medicine, One Baylor Plaza, Houston, TX 77030, USA; [5]Department of Pediatrics, Weill Cornell Medical College, 1300 York Avenue, New York, NY 10065, USA; [6]Graduate Program in Immunology and Microbial Pathogenesis, Weill Graduate School of Medical Sciences, Cornell University, 1300 York Avenue, New York, NY 10065, USA

CCL5 is a member of the CC chemokine family expressed in a wide array of immune and non-immune cells in response to stress signals. CCL5 expression correlates with advanced human breast cancer. However, its functional significance and mode of action have not been established. Here, we show that CCL5-deficient mice are resistant to highly aggressive, triple-negative mammary tumor growth. Hematopoietic CCL5 is dominant in this phenotype. The absence of hematopoietic CCL5 causes aberrant generation of CD11b$^+$/Gr-1$^+$, myeloid-derived suppressor cells (MDSCs) in the bone marrow in response to tumor growth by accumulating Ly6C^{hi} and Ly6G$^+$ MDSCs with impaired capacity to suppress cytotoxicity of CD8$^+$ T cells. These properties of CCL5 are observed in both orthotopic and spontaneous mammary tumors. Antibody-mediated systemic blockade of CCL5 inhibits tumor progression and enhances the efficacy of therapeutic vaccination against non-immunogenic tumors. CCL5 also helps maintain the immunosuppressive capacity of human MDSCs. Our study uncovers a novel, chemokine-independent activity of the hematopoietically derived CCL5 that promotes mammary tumor progression via generating MDSCs in the bone marrow in cooperation with tumor-derived colony-stimulating factors. The study sheds considerable light on the interplay between the hematopoietic compartment and tumor niche. Because of the apparent dispensable nature of this molecule in normal physiology, CCL5 may represent an excellent therapeutic target in immunotherapy for breast cancer as well as a broad range of solid tumors that have significant amounts of MDSC infiltration.

Keywords: CCL5; myeloid-derived suppressor cell; triple-negative breast cancer; immune response; mammary tumor; bone marrow; cytotoxic T lymphocyte
Cell Research (2013) 23:394-408. doi:10.1038/cr.2012.178; published online 25 December 2012

Introduction

CCL5 is a member of the CC chemokine family of proteins. It is expressed inT lymphocytes, platelets, macrophages, tubular epithelium, synovial fibroblasts, endothelial cells and selected tumor cells [1, 2]. CCL5 interacts with CCR1, CCR3, and CCR5 in various cell

types [3].

The human *CCL5* gene is located on the long arm of chromosome 17, the same area that Her2/neu is encoded and an area amplified in 30% breast cancer patients [4]. Tumor-derived CCL5 is detected in many clinical specimens of breast and cervical cancers; greater plasma levels in patients with progressive and more advanced disease than those in remission [5-7], and it constitutes a prominent part of a poor prognosis signature of inflammatory breast cancer [8, 9]. The concentration of CCL5 was significantly higher in the groups of patients with or without axillary lymph node metastasis [10]. CCL5

expression may be indicative of an ongoing, but as yet undetectable, malignant process [11]. In stage II patients, the expression of CCL5, the absence of estrogen receptor (ER)-α, and the lack of progesterone receptor (PR) expression significantly increased the risk of disease progression. Conversely, in the stage II group as a whole, the combinations of CCL5-negative/ER-α-positive and CCL5-negative/PR-positive were highly correlated with an improved prognosis [5].

In animal studies, tumor-derived CCL5 is able to upregulate transcription of matrix metalloproteinase-9, which contributes to tumor invasion and metastasis *in vivo* [12]. Systemic administration of Met-CCL5, a dominant-negative mutant of CCL5 and an antagonist of CCR1 and CCR5, is able to inhibit experimental breast tumor growth *in vivo* [13].

Consistent with its tumor-promoting role in breast cancer, CCL5, along with CCL2, has been shown to mediate many types of tumor-promoting cross-talks between the tumor cells and cells of the tumor microenvironment. It shifts the balance at the tumor site between different leukocyte cell types by increasing the presence of deleterious tumor-associated macrophages (TAM) and inhibiting potential anti-tumor T-cell activities. CCL5 expressed by cells of the tumor microenvironment osteoblasts and mesenchymal stem cells plays a role in breast cancer metastatic processes. In addition, CCL5 acts directly on the tumor cells to promote their pro-malignancy phenotype by increasing their migratory and invasion-related properties [14].

Despite the large amount of correlative and *in vitro* studies, the role of CCL5 and the mechanisms involved in its tumor-promoting property have not been directly demonstrated *in vivo*. One recent study suggests that tumor-derived CCL5 expression does not make a significant contribution to mammary carcinoma growth [15]. We thus hypothesized that non-tumor-derived CCL5 may play a critical role in promoting breast cancer progression. In the present study, we sought to directly address this issue by utilizing the syngeneic, ER-α/PR/Her2/neu-negative (triple-negative) 4T1 mammary carcinoma model in CCL5 knockout (KO) mice.

Results

Reduced primary tumor growth and metastatic disease in CCL5 KO mice

To assess the effects of the host-derived CCL5 on tumor growth, female BALB/c wild-type (WT) and CCL5-KO mice were inoculated in the mammary gland with syngeneic 4T1 mammary carcinoma cells [16], which spontaneously produce CCL5 [12]. CCL5 KO mice,

which are developmentally normal by some key features, were resistant to 4T1 tumor growth with a mean tumor size of ~8 mm in diameter versus 17 mm in control WT mice on day 25 (Figure 1A). When the tumor size reached 15~20 mm in diameter, lung metastases were compared between WT and KO mice. There were far fewer lung metastases in KO mice (Figure 1B), reiterating that host-derived CCL5 plays a dual role in promoting 4T1 tumor growth and lung metastasis.

A previous study showed high incidence and intensity of CCL5 expression in breast cancer cells associated with more advanced disease stages [11]. This observation raised a question about the cellular source of CCL5, i.e., cancer cells, host cells, or both, that is important for tumor progression. To address this question, we used a variant of the 4T1 tumor in which endogenous CCL5 expression was stably silenced via siRNA [15]. The efficiency of the knockdown of CCL5 was confirmed by real-time PCR (Supplementary information, Figure S1). The variant 4T1(siCCL5) was injected into WT and CCL5 KO mice. Figure 1C shows that in both WT and KO mice, 4T1(siCCL5) grew similarly to the non-specific siRNA-transfected control cell line 4T1(siNS). Examination of serum CCL5 levels in WT and KO mice before and after bearing 4T1(siNS) or 4T1(siCCL5) tumor at an early phase (10 days post tumor inoculation) and late phase (20 days) indicated that the bulk of the circulating CCL5 came from the host, not the tumors (Figure 1D). These data suggest that tumor-derived CCL5 does not play a major role in 4T1 tumor progression, consistent with the findings of a previous study [15].

The hematopoietic compartment is the source of immune cells expressing CCL5, including T cells, platelets and macrophages [17]. CCL5 has chemotactic activity by directing immune cells, especially T cells and monocytes, to the site of inflammation and infection [2]. To determine the relative importance of the origin of CCL5 expression, hematopoietic versus non-hematopoietic compartments, that contributes to the tumor-resistant phenotype observed in CCL5 KO mice, we performed reciprocal bone marrow transplants into WT and KO recipients, and then subjected them to 4T1 tumor challenge. All female transplant recipient mice displayed successful hematopoietic engraftment based on the presence of the Y chromosome gene product (from male donors) in splenocytes (Supplementary information, Figure S2). As shown in Figure 1E, transplantation of KO marrow inhibited tumor growth in WT recipients, while transplanting WT marrow into KO recipients promoted tumor growth in KO recipients (Figure 1F). The metastasis data showed the same trend as tumor growth (Supplementary information, Figure S3). Together, these data confirm
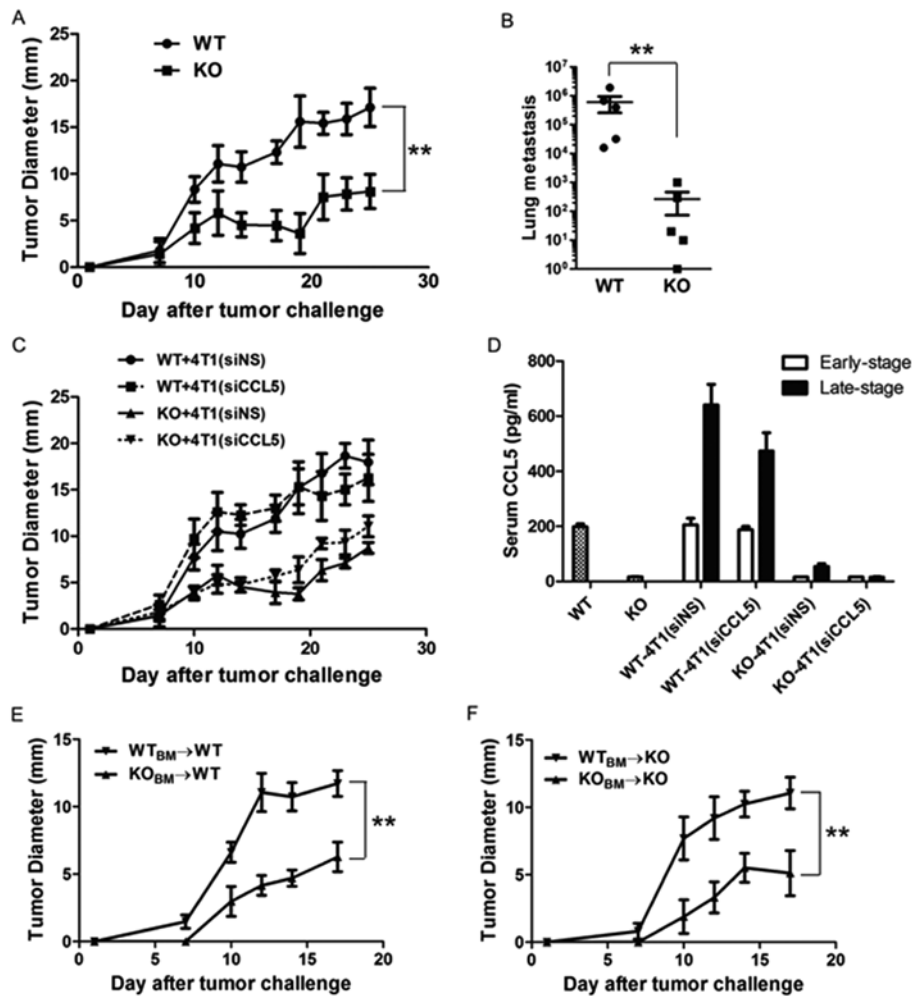
Figure 1 4T1 tumor growth and metastasis in CCL5 KO mice. **(A)** 4T1 tumor cells were injected into the mammary gland of female WT and KO mice. Tumor growth was monitored every 2-3 days. Data are represented as mean ± SE. Each group contained five mice. **(B)** Lung metastasis of 4T1 tumor cells was measured by the 6-thioguanine clonogenicity assay. When tumor diameter reached 20 mm, mice were sacrificed and the number of lung metastasis was quantified. **(C)** Tumor growth in WT and KO mice injected with control cell line 4T1(siNS) or 4T1(siCCL5). $n = 5$ mice per group. **(D)** 10 days (early stage) or 20 days (late stage) after tumor cell inoculation, mice were sacrificed and serum was collected for measurement of CCL5 protein by ELISA. $n = 5$ mice per group. **(E, F)** Lethally irradiated female WT and KO mice were transplanted with male WT **(E)** and KO **(F)** bone marrows. Thirty days after bone marrow reconstitution, the recipients were inoculated with 4T1 cells and tumor growth was monitored every 2-3 days. Data are represented as mean ± SE. Each group contained three mice. **$P < 0.01$.

that deficiency of hematopoietic CCL5, rather than those from peripheral tissues and tumor cells, is the primary basis for the phenotype of CCL5 KO mice.

Aberrant phenotype of myeloid-derived suppressor cells (MDSCs) in CCL5 KO mice

To further understand the cellular mechanisms involved in 4T1 tumor progression, we analyzed by flow cytomery the major subsets of leukocytes in the spleen of mice bearing the tumor and those that infiltrated the tumor: $CD4^+$ and $CD8^+$ T cells, $CD4^+$, $CD25^+$, $Foxp3^+$ T regulatory cells (Tregs), $CD3^+$ $NK1.1^+$ NKT cells, $CD11b^+/Gr-1^+$ myeloid cells, all of which are highly relevant to the regulation of tumor growth. Initial analyses indicated that the compositions of most cell types were not significantly altered between WT and CCL5 KO mice in the spleen and in the tumor (TIC), except for the lower frequency of Tregs infiltrated into the tumors in KO mice (Figure 2A iii). We also examined the number of TAM in WT and KO mice, and no statistical difference was observed (Supplementary information, Figure S4).

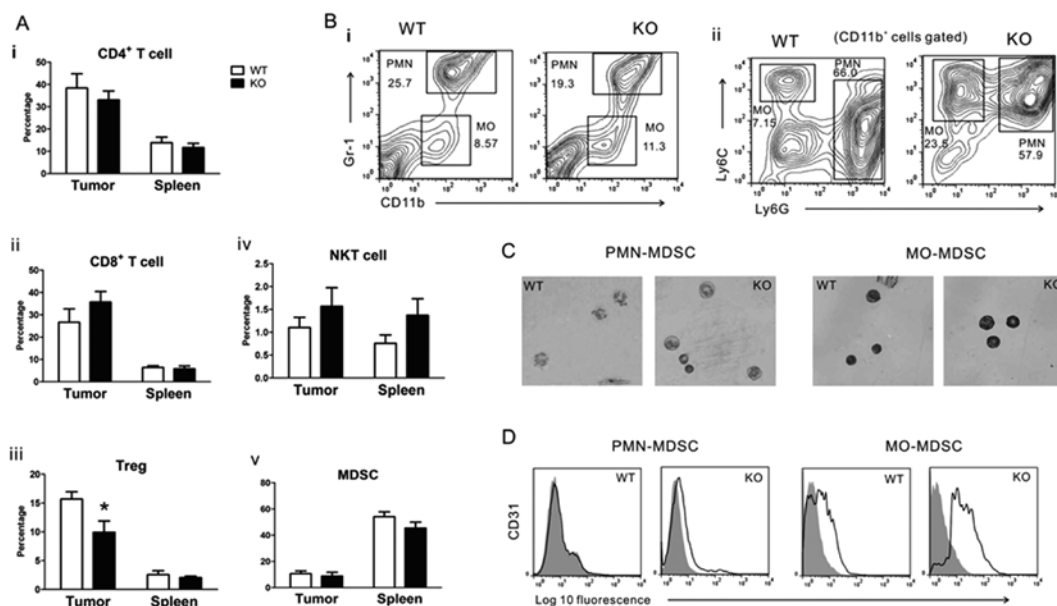Further examination revealed some "subtle" changes

Figure 2 Aberrant differentiation of MDSCs in CCL5 KO mice. **(A)** At 2 weeks after 4T1 cell inoculation, tumor-infiltrating cells and splenocytes from WT and KO mice were analyzed by flow cytometry. Percentages of CD4+ T cells (i), CD8+ T cells (ii), Treg cells (iii), NKT cells (iv), and CD11b+ Gr-1+ cells (v) are indicated with mean and SD. **(B)** Splenocytes from tumor-bearing WT and KO mice were stained for expression of CD11b and Gr-1(i); the CD11b+ subset was further analyzed for Ly6G versus Ly6C expression (ii). **(C)** Sorted MDSC subsets were stained with May-Grünwald Giemsa to evaluate their morphology. Original magnification, 400×. **(D)** Sorted MDSC subsets were stained for CD31 expression. *$P < 0.05$. $n = 5$ mice per group.

in the subset of CD11b+/Gr-1+ myeloid cells, which are known as MDSCs (Figure 2B i). CD11b+/Gr-1+ MDSCs can be further separated into two major subsets on the basis of the differential expression of the antigens Ly6G and Ly6C, polymorphonuclear (PMN)-MDSCs expressing Ly6G and monocytic (MO)-MDSCs expressing Ly6C. These two subsets may have different immunosuppressive activities via different mechanisms in cancer and infectious diseases [18-21]. As shown in Figure 2B ii, the MDSCs in the spleens of KO mice displayed some altered features, based on staining with Ly6G and Ly6C, in that they became less "polarized" with respect to Ly6C and Ly6G expression. In other words, the PMN subset became double positive in the absence of CCL5, while the MO subset of KO mice had lower Ly6C expression at a higher frequency compared to that of WT mice.

To further investigate the characteristics of the MDSC subsets, we purified these cells by microbeads (see Supplementary information, Figure S5 for details), and examined them microscopically by May-Grünwald Giemsa staining (Figure 2C). The PMN subset from WT mice were mainly composed of mature polymorphonuclear cells with segmented ring-shaped nuclei and faint to invisible cytoplasm. In contrast, the PMN subset from KO mice displayed a visible and bluer cytoplasm and

pleiomorphic nuclei. The MO subset from WT mice was heterogeneous in size, whereas the MO subset of KO mice was composed of mostly immature mononuclear cells or myeloid precursors with doughnut-shaped nuclei [18].

Since the morphological data showed changes in the maturation state of MDSCs in KO mice, we next tried to test whether there was differential expression of other maturation-related surface markers. However, there was no dramatic difference between WT and KO mice in the expression of F4/80 and CD115, which were weakly expressed in the MO subset of both WT and KO mice (data not shown). The only discernible change was the expression of CD31, the vascular adhesion molecule platelet endothelial cell adhesion molecule 1 (PECAM-1), which was also the marker of immature hematopoietic precursors [22, 23]. Both the MO and PMN subsets from KO mice had higher CD31 expression (Figure 2D). The levels of CD31 expression in different subsets were shown in Supplementary information, Figure S6.

Impaired function of CCL5-deficient MDSCs in vitro

The altered phenotype of the MDSC subsets in CCL5 KO mice prompted us to determine whether the function of the MDSC subsets, i.e., their hallmark immuno-

suppressive activity, was also altered. Purified MDSC subsets from WT and KO mice were added in different radios to the TCR transgenic CL4 splenocytes in the presence of the antigenic peptide HA$_{512-520}$, and antigen-specific T cell proliferation was measured. The MO-MD-SCs of WT mice strongly suppressed T-cell proliferation dose dependently, whereas those of KO mice displayed much reduced activity (Figure 3A). The PMN-MDSCs of WT mice exhibited weak T-cell-inhibiting activity, and those of KO mice were slightly more suppressive (Figure 3B). Next, we used ELISPOT assays for IFNγ production by T cells to evaluate the effect of MDSC subsets on the function of T cells. The results showed that the MO subset in WT mice exhibited statistically significant suppressive activities, while the MO subset from KO mice only induced a slight decrease in the number of IFNγ-specific spots (Figure 3C). Weakly decreased number of IFNγ-producing cells could be seen in PMN groups from both WT and KO mice, but it did not reach statistical significance (Figure 3C). Consistent with these observations, we found that the MO subset of KO mice displayed much reduced activity of a key enzyme in the arginine metabolism pathway and an important constituent of the immunosuppressive property of MDSCs [24], iNOS, (Supplementary information, Figure S7A), due to impaired gene transcription (Supplementary information, Figure S7B).

Although our results demonstrated that MDSCs in CCL5 KO mice, particularly the MO subset, lost the immunosuppression activity on both antigen-specific T-cell proliferation and IFNγ production *in vitro* (Figure 3A and 3C), we did not observe significant difference between WT and KO tumor-bearing mice in the number of CD8$^+$ T cells from either spleens or tumors (Figure 2A). To further address this question, we collected splenocytes from WT and KO mice that had been inoculated with 4T1 cells 2 weeks before, and restimulated them with irradiated 4T1 cells. IFNγ-specific ELISPOT assay showed that T cells from KO mice mounted stronger response against tumor antigens than their WT counterparts (Figure 3D).

Contribution of defective MDSCs to reduced tumor progression in CCL5 KO mice
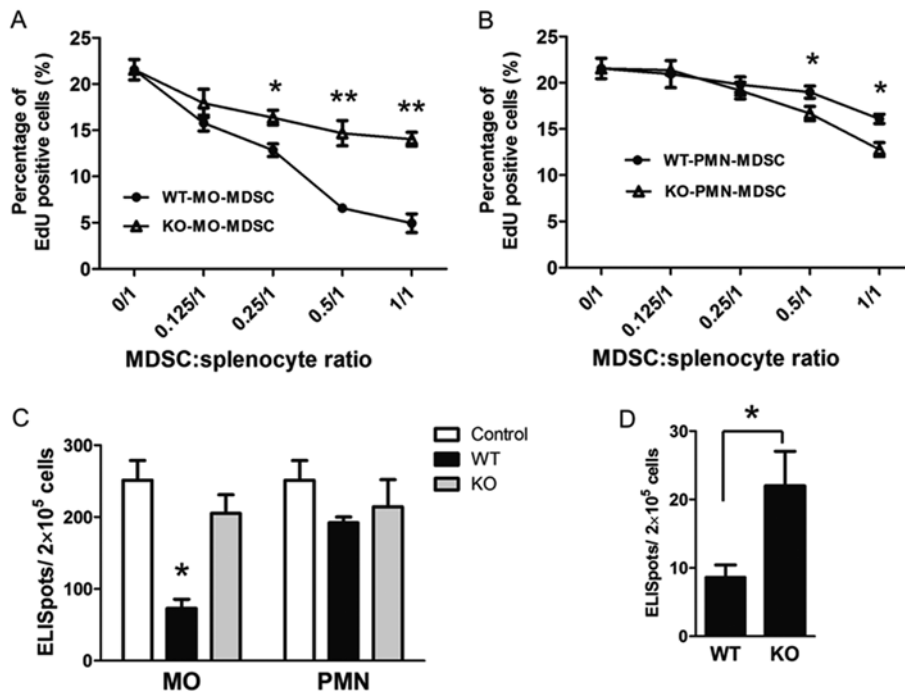
To determine whether the enhanced antitumor activity

Figure 3 Functional impairment of CCL5-deficient MDSCs *in vitro*. **(A, B)** Splenocytes from CL4 transgenic mice stimulated *in vitro* with 1 μg/ml of HA$_{512-520}$ peptide were cultured with various amounts of purified MO-MDSCs **(A)** or PMN-MDSCs **(B)** from CCL5 WT or KO mice. Percentages of proliferating cells were determined by flow cytometry (*n* = 3). **(C)** ELISPOT analysis for IFNγ production by activated T cells in the same experimental setup as in **A**. The ratio of MDSCs to CL4 splenocytes was 1:4. **(D)** Tumor-specific IFNγ production by T cells. Splenocytes from 4T1 tumor-bearing WT and KO mice were incubated with irradiated 4T1 cells for 48 h. IFNγ production by T cells was assessed by ELISPOT. Data are represented as mean ± SE. Each group contained five mice. *$P < 0.05$; **$P < 0.01$.

in CCL5 KO mice was dependent on the impairment of MDSCs, we performed adoptive transfer experiments. The CD11b$^+$, Gr-1$^+$ MDSCs were isolated from the spleen of 4T1 tumor-bearing WT or KO mice, and transferred to recipient WT and KO mice inoculated with 4T1 tumor cells. As shown in Figure 4A, 3 weeks after the inoculation, the tumor volume of KO mice receiving adoptive transfer of functional WT MDSCs increased almost 2-fold, whereas that of KO mice receiving KO MDSCs was similar to the tumor size in KO mice that did not receive adoptive transfers. The tumor growth patterns were echoed in tumor metastasis to the lung (data not shown).

Since there was a lower frequency of Tregs in TILs and greater tumor-specific T-cell response in CCL5 KO mice (Figure 2A iii and 3D), we further assessed whether these immune properties were altered after adoptive transfer of MDSCs. As shown in Figure 4B and 4C, after transfers of WT MDSCs, the number of tumor antigen-specific IFNγ-producing cells was decreased and the frequency of tumor-infiltrated Tregs was increased in KO mice, reducing the significant differences between WT and KO mice.

These data suggest that the impaired function of the MDSCs, including the suppressive effect on T-cell responses and the induction of Tregs, underlines the re-

duced tumor growth and metastasis in CCL5 KO mice.

Plasma CCL5 levels in breast cancer patients were previously found to be associated with progression of the disease from stage II to stage IV without identifying the producers of CCL5 [6]. Our experimental data demonstrated that host-derived CCL5 contributes to higher serum CCL5 levels in the 4T1 tumor model (Figure 1D). These observations did not address the question whether tumor-infiltrating cells of host origin contributed to the high serum levels of CCL5 in the host. To answer this question, we isolated tumor cells and MDSCs from primary tumors and spleen after 10 days (early stage) and 20 days (late stage) post tumor inoculation, and measured CCL5 mRNA levels. As shown in Figure 4D, CCL5 mRNA expression was not significantly increased between early and late stages in tumor cells from either WT or KO mice. In contrast, CCL5 mRNA levels were dramatically enhanced in both tumor-infiltrating and splenic MDSCs of WT mice after 20 days of tumor inoculation (Figure 4E). At the same time, we also found that the amount of tumor-infiltrating and spleen MDSCs were increased with the disease progression (Supplementary information, Figure S8). The CCL5 mRNA expression data were also recapitulated at the protein level (Supplementary information, Figure S9). These data clearly
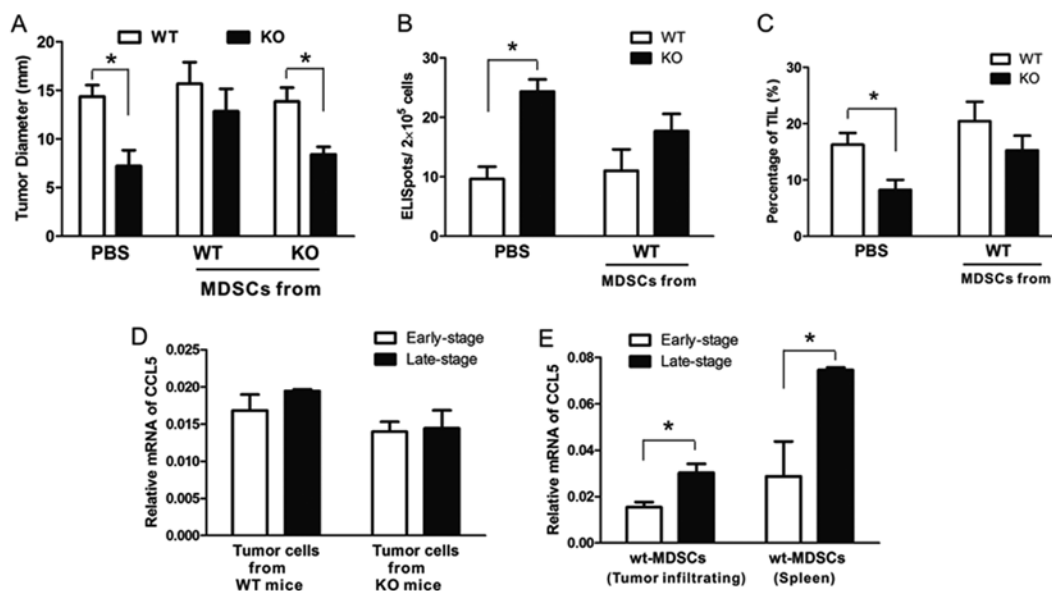

Figure 4 Contribution of defective MDSCs to weakened tumor progression in CCL5 KO mice. **(A)** WT and CCL5 KO mice were inoculated s.c. with 4T1 tumor cells, then were divided into three groups (5 mice per group), and were injected i.v. with or without MDSC cells from WT or CCL5 KO mice. Tumor size was measured 25 days after 4T1 inoculation. **(B**, **C)** Tumor-specific IFNγ-producing spots **(B)** and tumor-infiltrating Treg cells **(C)** from CCL5 WT and KO mice (*n* = 3) that had received the adoptive transfer of WT MDSCs were measured by ELISPOT and flow cytometry, respectively. **(D**, **E)** Total RNA was extracted from separated tumor cells **(D)** and MDSCs **(E)**, and CCL5 mRNA level was measured by quantitative RT-PCR. *$P <$ 0.05.

demonstrate that MDSC-derived CCL5 contributes to higher serum CCL5 levels in the late stage of 4T1 tumor model.

Amplification of intrinsically defective bone marrow differentiation in CCL5 KO mice by tumor growth

Because the tumor growth-inhibiting phenotype of CCL5 KO mice was dependent on the impaired activity of the MDSCs, we further explored the mechanism whereby CCL5 impacts the change in the MDSC subsets.

CCL5 is a chemokine that can direct the migration of several types of immune cells to inflammatory sites [1]. We first asked whether changes in MDSC subsets observed in peripheral tissues in CCL5 KO mice were due to the disrupted cellular migration. We systematically analyzed the $CD11b^+$, $Gr-1^+$ cells in the tumor, spleen and bone marrows of WT and KO mice by the expression of Ly6G and Ly6C. As shown in Figure 5A, these cells present in the tumor (left), the spleen (middle), and the bone marrow (right) displayed very similar phenotypic patterns but merely different between WT and KO mice, suggesting that cellular migration was not the cause of the phenotypic change in KO mice. In other words, there were intrinsic differences in the MDSC between WT and KO mice that originated in the bone marrow. In addition, the phenotypic differences in MDSC subsets between WT and KO mice were not caused by the specific tumor type because another mammary tumor cell line, DA3 [25], when inoculated into mice, induced similar types of MDSCs (Supplementary information, Figure S10).

Further analyses of bone marrow cells from tumor-bearing mice staining with CD31 and Ly6C revealed six phenotypically distinct subsets, which had previously been described by others [26, 27]. The $CD31^{hi} Ly6C^-$ subset consists predominantly of undifferentiated blast cells (Bl). The $CD31^+ Ly6C^+$ subset contains a large proportion of morphologically undifferentiated blasts, together with recognizable precursors of the myeloid, erythroid and lymphoid lineages (Bl&P). The $CD31^- Ly6C^{hi}$ subset is composed of mainly monocytes and some immature myeloid cells (M). The $CD31^- Ly6C^{med}$ subset is highly enriched for granulocytes (G). The $CD31^- Ly6C^-$ subset consists almost exclusively of erythroid cells, erythroblasts as well as more mature cells (E). Finally, the $CD31^{med} Ly6C^-$ subset is highly homogenous with predominantly mature lymphoid cells (L).

Our analyses showed that bone marrows from tumor-bearing mice harbored large numbers of myeloid cells but lost almost all of the mature erythrocytes and lymphocytes (Figure 5B and 5C). Notably, there were two dramatic changes in KO mice: (1) the granulocytes had higher Ly6C expression, and most cells were located at the border between the G and M regions; (2) more cells accumulated in the Bl&P region concomitant with much fewer cells in the Bl region. These alterations were already present in steady state (tumor-free) between WT and KO mice in the bone marrow (Supplementary information, Figure S11A and S11B), except that tumor growth resulted in the amplification of the differences in MDSC subsets, and in the loss of the L and E subsets.

To further elucidate the basis of the altered myelopoiesis in KO mice, we analyzed $CD11b^+$ cells from the bone marrow from tumor-bearing mice for expression of Ly6G, Ly6C and CD31. In WT mice, the $Ly6C^+$ cells are mainly from the M subset, and $Ly6G^+$ cells from the G subset. In KO mice, the main source of $Ly6C^+$ cells was the Bl&P region while the granulocyte subset ($Ly6G^+$ $Ly6C^+$) were composed of cells from the G, M and Bl&P regions (Figure 5D).

Our findings are consistent with the established notion that expansion of MDSCs is mediated by tumor-derived factors through stimulating myelopoiesis in the bone marrow and inhibiting the differentiation of mature myeloid cells [24]. To directly demonstrate the role of hematopoietic CCL5 in the regulation of myelopoiesis, we performed adoptive transfers of bone marrow derived from WT and KO mice into KO mice. Following reconstitution of hematopoiesis in recipient mice, they were challenged with 4T1 tumor cells. Splenocytes and bone marrow were assessed by flow cytometry 2 weeks after tumor inoculation. Transplantation of WT marrow into KO mice restored normal MDSC subsets (Figure 5E, left) and normal myelopoiesis (Figure 5E, left). In contrast, transplantation of KO marrows did not "rescue" these alterations in KO recipient mice (Figure 5E, right panels). Data from the reciprocal bone marrow transfers were consistent with the theme (Supplementary information, Figure S12). Therefore, hematopoietic CCL5 plays a dominant role in regulating MDSC differentiation.

Functional cooperation between CCL5 and tumor-derived factors in generation of MDSCs

Our observation of an impaired generation of MDSCs in the bone marrow of CCL5 KO mice in response to tumor growth prompted us to further identify tumor-derived factors involved in the process. Previous studies have identified two cytokines, granulocyte and macrophage colony-stimulating factor (GM-CSF) and macrophage colony-stimulating factor (M-CSF) as important contributors in the expansion of MDSCs [18, 28, 29]. To determine the functional relationship of CCL5 with these myeloid colony-stimulating factors, we compared the colony-forming activity of WT and KO bone marrow progenitor cells in the presence of GM-CSF, M-CSF and
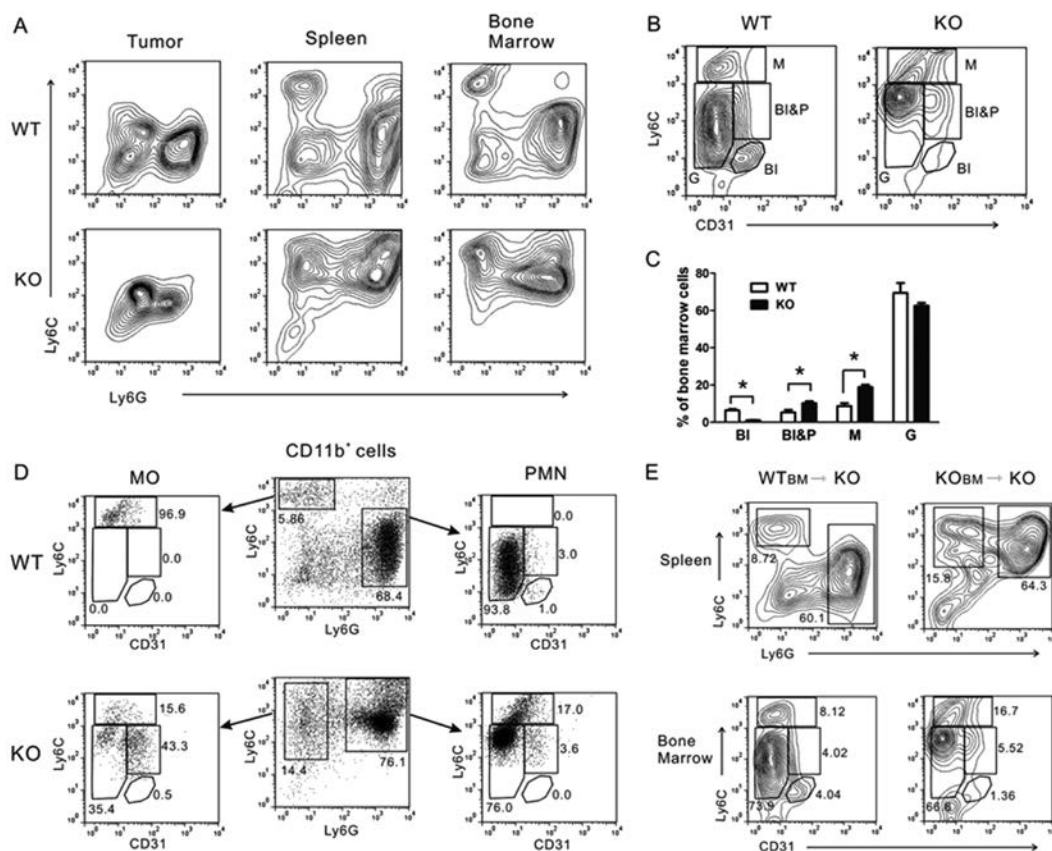
Figure 5 Tumor-augmented alterations in bone marrow differentiation in CCL5 KO mice. **(A)** CD11b^{+} cells from bone marrow, spleen and tumor of WT and CCL5 KO mice were analyzed by flow cytometry for the presence of Ly6G and Ly6C markers. **(B)** Whole bone marrow cells were isolated from tumor-bearing WT and CCL5 KO mice and subjected to flow cytometry for CD31 and Ly6C expression. Bl, blasts; P, progenitors; M, monocytes; G, granulocytes; L, lymphocytes. **(C)** Quantification of different subsets in **B**. *$P < 0.05$. **(D)** Whole bone marrow cells were isolated from tumor-bearing WT and KO mice and subjected to flow cytometry for expression of CD31, CD11b, Ly6G and Ly6C. The MO and PMN subsets in bone marrow (gated on CD11b^{+} cells) were analyzed by CD31 and Ly6C expression to determine their origins. **(E)** Lethally irradiated KO recipient mice (female) were reconstituted with bone marrow from WT or KO donor mice (male). Thirty days after hematopoietic reconstitution, recipient mice were inoculated with 4T1 cells. After 2 weeks, splenocytes and bone marrow cells from tumor-bearing KO recipient were analyzed by flow cytometry for MDSC phenotypes. n = 5 mice per group.

G-CSF. As shown in Figure 6A, treatment with GM-CSF elicited a higher number of colonies from KO bone marrow cells than from WT bone marrow cells, particularly at lower concentrations. Microscopic examination indicated that colonies formed from KO bone marrow cells were mainly composed of monocytes rather than granulocytes (data not shown). Similarly, stimulation of KO bone marrow cells with M-CSF resulted in higher numbers of colonies than in WT bone marrow (Figure 6B). In contrast, stimulation of KO cells with G-CSF caused no difference between WT and KO cells, except at the highest concentration (100 ng/ml) (Figure 6C).

ELISA analyses showed that GM-CSF, M-CSF and G-CSF levels in tumor-bearing mice were about 0.25, 1.5 and 8.5 ng/ml, respectively (Supplementary information,

Table S1), and the concentration were not significantly different between WT and KO mice, suggesting that although CCL5 alone does not directly promote colony formation of bone marrow progenitors (data not shown), it regulates GM-CSF- and M-CSF-, but not G-CSF-induced myeloid differentiation. These results demonstrated that the absence of CCL5 skews the differentiation of the myeloid precursors towards the monocytic lineage in the presence of GM-CSF and M-CSF.

To investigate functional interactions between tumor-secreted GM-CSF and M-CSF with CCL5 *in vivo* in the induction of MDSCs and in the regulation of tumor growth, we inoculated WT and KO mice with 4T1 cells in which expression of the endogenous GM-CSF and M-CSF were stably knocked down via hsRNAs (Supple-
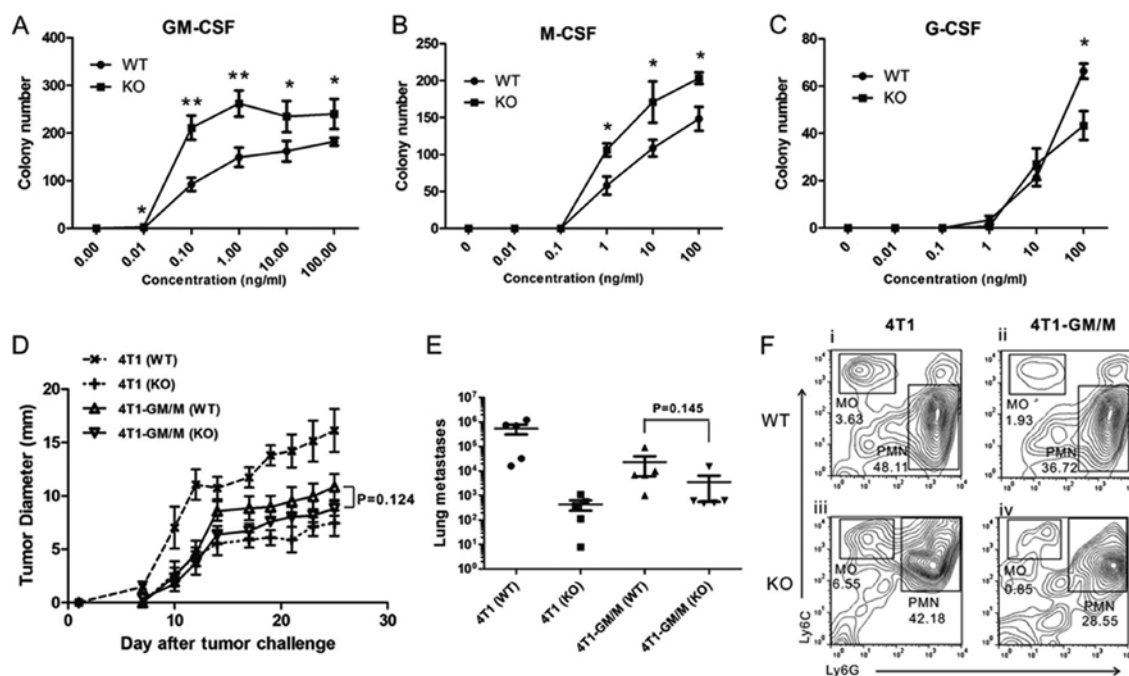
Figure 6 Role of tumor-derived GM-CSF, M-CSF and G-CSF. **(A-C)** Colony formation from bone marrow cells from WT and KO mice in response to cytokine. Single-cell suspensions from bone marrow from WT and KO mice were plated in methylcellulose in the presence of the indicated amounts of GM-CSF **(A)**, M-CSF **(B)** and G-CSF **(C)**. The results are representative of three independent experiments. *$P < 0.05$; **$P < 0.01$. **(D)** 4T1 and 4T1-GM/M tumor cells were injected into the mammary gland of female WT and KO mice. Tumor growth was monitored every 2-3 days. Data are represented as mean ± SE. Each group contained five mice. **(E)** Lung metastasis of tumor cells was measured. **(F)** Flow cytometry analysis of MDSCs (gated on CD11b$^+$ cells) in spleens from 4T1- or 4T1-GM/M-inoculated mice, for Ly6G and Ly6C markers. Numbers in contours indicate the percentage of total MDSCs in the corresponding gates.

mentary information, Table S2). Knocking down the expression of both GM-CSF and M-CSF in 4T1 cells (4T1-GM/M) resulted in slower tumor growth in WT mice compared to the parental tumor, whereas tumor growth was slightly accelerated in KO mice. But there was no significant difference between WT and KO mice bearing 4T1-GM/M tumors (Figure 6D). Likely because of the residual amounts of GM-CSF and M-CSF expressed by 4T1-GM/M, tumor growth was still slightly inhibited in KO mice compared to WT mice. However, no statistical significance between these two groups was observed. Lung metastasis in 4T1-GM/M-inoculated mice had the same tendency as tumor growth (Figure 6E). The slower growth of 4T1-GM/M cells *in vivo* was not due to intrinsic properties, since they exhibited similar proliferative rates *in vitro* to parental 4T1 cells (Supplementary information, Figure S13). Analysis of MDSCs in spleens of tumor-bearing mice showed that the immunosuppressive MO subset (Ly6C$^+$, Ly6G$^-$) was substantially reduced in WT mice bearing 4T1-GM/M compared to those bearing 4T1 and patterns of MDSCs in KO mice bearing 4T1-GM/M is similar to WT mice, confirming that tumor-

derived GM-CSF and M-CSF play an important role in the induction of MO-MDSCs, and that CCL5 could not affect the expansion of MDSCs without GM-CSF and M-CSF but it cooperates with them *in vitro* and *in vivo* (Figure 6F).

Antibody blockade of CCL5 inhibits tumor growth and improves the efficacy of therapeutic vaccination

Tumor immunosuppression is one of the major factors responsible for the failure of cancer vaccines, and recent studies have identified MDSCs as one of the important elements in tumor immunosuppression [30]. 4T1 tumor is notoriously non-immunogeneic when used in immunization. To determine whether inhibition of CCL5 could improve the efficacy of therapeutic vaccination against 4T1 tumor, we injected irradiated 4T1 cells together with a CCL5-neutralizing mAb into mice inoculated with live 4T1 cells. Injection of anti-CCL5 alone slowed down tumor growth (Figure 7A) and reduced lung metastasis (Figure 7B). However, injection of irradiated 4T1 cells and the anti-CCL5 mAb together gained greater efficacy in both aspects.

To further corroborate these results, we evaluated the tumor-specific immune response following vaccination of mice by ELISPOT. Splenocytes from mice injected with irradiated 4T1 cells or irradiated 4T1 cell plus control antibody did not respond to tumor-specific antigen, compared to control group (Figure 7C). In contrast, a significant number of antigen-specific IFNγ-producing T cells were found in the spleens of mice infected with irradiated 4T1 cell plus the CCL5 mAb.

These data suggest that therapeutic vaccination via neutralizing CCL5 may be an effective strategy for treating advanced TNBC.

Spontaneous mammary tumors exhibit similar MDSC and CCL5 phenotypes

Spontaneous murine mammary carcinoma can be induced by oncogene overexpression in the mammary gland such as Wnt-1, which was first identified as a protooncogene activated by viral insertion in mouse mammary tumors (MMTV-Wnt1). The potent mitogenic effect mediated by Wnt-1 expression does not require
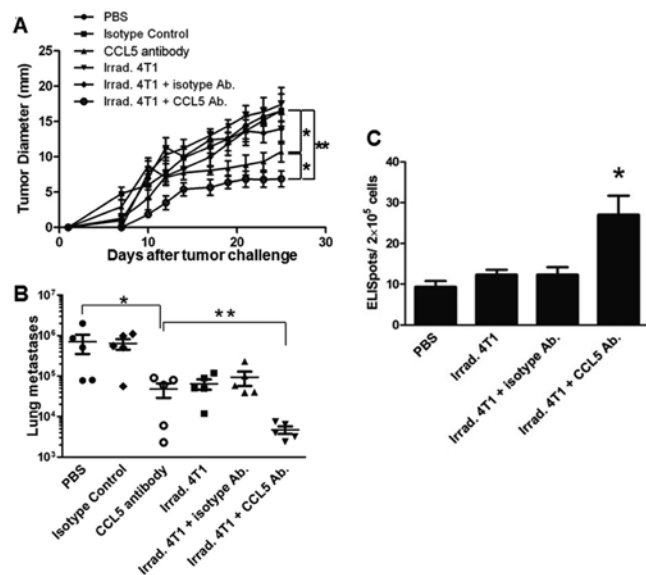

Figure 7 Effect of antibody-mediated blockade of CCL5 on tumor growth and therapeutic vaccination efficacy. **(A**, **B)** Therapeutic vaccination: mice were injected i.p. with irradiated 4T1 cells or PBS on days 3, 7 and 10, accompanied by injection of anti-CCL5 mAb or control IgG on days 7 and 14. Tumor size **(A)** and lung metastasis **(B)** were measured 25 days post tumor cell inoculation. **(C)** Tumor antigen-specific immune response in treated mice. Splenocytes from 4T1 tumor-bearing mice (treated as described in **A**) were incubated with irradiated 4T1 cells for 48 h. IFNγ production by T cells was assessed by ELISPOT. Data are represented as mean ± SE. *$P < 0.05$; **$P < 0.01$. $n = 5$ mice per group.

estrogen stimulation; tumors form after an increased latency in ER-α-null mice [31]. Several genetic lesions, including inactivation of p53 and over-expression of Fgf-3, collaborate with Wnt-1 in leading to mammary tumors [31].

To compare the characteristics of MDSCs and CCL5 expression between 4T1 and MMTV-Wnt1-induced mammary tumors, we first analyzed the amount of MDSC infiltration in two types of tumors. As shown in Figure 8A, there were considerable amount of CD11b+, Gr-1+ MDSCs in the Wnt1 tumor (~4%), although less than the 4T1 tumor (~9%). However, compared to tumor-free mice, Wnt1 tumor-bearing mice had > 5-fold more MDSCs present in their spleens (Figure 8B). Moreover, compared to tumor cells, the MDSCs expressed > 5-fold more CCL5 mRNA on a per cell basis (Figure 8C). More importantly, splenic MDSCs from the Wnt1 tumor-bearing mice also expressed much higher levels of immunosuppressive molecules such as iNOS (Figure 8D), TGF-β (Figure 8E) than those from the tumor-free mice, while arginase 1 levels were comparable (Figure 8F).

These data demonstrate that MDSC development and tumor infiltration as well as the expression of CCL5 and key immunosuppressive factors by MDSCs are associated with spontaneous mammary tumors, and not a peculiar feature of the orthotopic 4T1 model.

Human CCL5 is required to maintain the suppressive function of MDSCs

In humans, suppressive CD33+ cells can be generated *in vitro* from PBMCs by GM-CSF and IL-6, and these cells are functionally consistent with MDSCs in immunosuppressive activity, morphology, surface phenotype and gene expression profile [32]. We cultured PBMCs from healthy volunteers in the presence of GM-CSF and IL-6 for 7 days. A dramatic increase in the frequency of MDSCs (CD33+ HLA-DR− CD3−) was observed in the GM-CSF and IL-6-treated groups; however, this effect was not significantly reduced after antibody-mediated blockade of CCL5 (Figure 8G). The MDSCs were then isolated by anti-CD33 microbeads and tested for suppressive function in inhibiting autologous T-cell proliferation at a ratio of 1:2. Figure 8H shows that GM-CSF and IL-6-induced MDSCs inhibited autologous T-cell proliferation by almost 70%, while this immunosuppression was reduced to 30% after blockade of CCL5. These data suggest that human CCL5 plays an important role in maintaining the immunosuppressive activity of MDSCs.

Discussion

MDSCs represent a heterogeneous population of cells

comprised of myeloid progenitors and immature myeloid cells that contribute to negative regulation of immune responses to malignant growth [24]. Previous studies have shown in various mouse models that depletion of MDSCs from tumors or spleens restores anti-tumor T-cell responses [33-38]. The accumulation of MDSCs is influenced by disturbances of cytokine homeostasis in pathological conditions, which stimulate myelopoiesis and inhibit the differentiation of mature myeloid cells [24]. Our study shows that hematopoietic CCL5 plays a pivotal role in the generation of MDSCs, and its absence alters the differentiation of MDSCs and decreases their immunosuppressive activity.

Recently, MDSCs have been defined more precisely in mice by two epitopes recognized by the Gr-1 antibody, Ly6G and Ly6C. Normally, CD11b$^+$ Ly6G$^-$ Ly6C^{hi} MD-SCs have monocytic phenotype, whereas CD11b$^+$ Ly6G$^+$ Ly6C^{low} MDSCs are of granulocytic phenotype [24]. Our analysis demonstrated that both the MO and PMN subsets from CCL5 KO mice have altered cell morphology, and the MO subset consists of myeloid precursor cells with doughnut-shaped nuclei [18], while the PMN subset from CCL5 KO mice look like the "atypical granulocytes", consistent with the literature [39]. Importantly, these two subsets have different functions in cancer, infectious and autoimmune diseases. Furthermore, they invoke distinct mechanisms to suppress T-cell function [24]. The MO subset expresses higher levels of iNOS and its suppressive activity depends on NO, whereas that of the PMN subset depends on arginase 1 [4]. Consistent with these observations, we showed that the MO subset from WT mice strongly suppressed antigen-specific CD8$^+$ T-
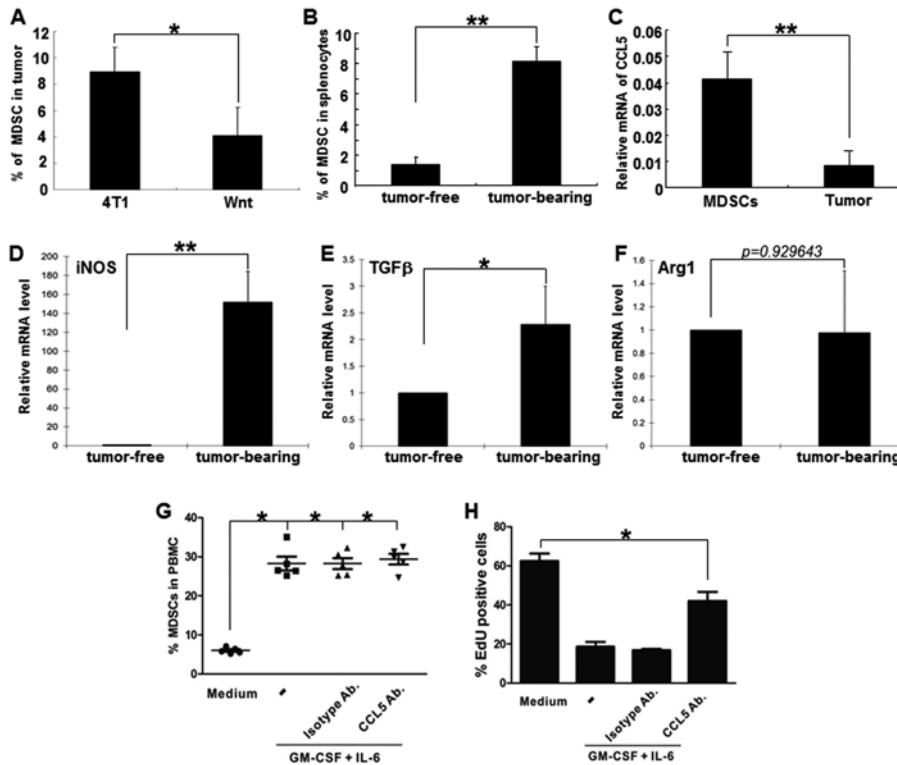

Figure 8 Characterization of MDSCs in MMTV-Wnt1 mammary tumors and from human peripheral blood. Tumors were collected from the MMTV-Wnt1 transgenic mice (4×) when they reached 1.5-2.0 cm in diameter, along with spleens and bone marrows, and analyzed by FACS for CD11b$^+$, Gr-1$^+$ MDSCs and by real-time PCR for mRNA expression levels of various molecules. **(A)** Percentages of MDSCs infiltrating 4T1 and Wnt1 tumors; **(B)** percentages of MDSCs in the splenocytes of tumor-free and Wnt1 tumor-bearing mice; **(C)** relative CCL5 mRNA levels in Wnt1 tumor cells and the tumor-infiltrating MDSCs; **(D-F)** relative mRNA levels in splenic MDSCs from tumor-free and Wnt1 tumor-bearing mice, respectively, for iNOS **(D)**, TGF-β **(E)**, and arginase 1 (Arg1) **(F)**. **(G)** The frequency of MDSCs, defined as CD33$^+$HLA-DR$^-$ CD3$^-$, is shown in the PBMCs of healthy donors cultured in the presence of GM-CSF plus IL-6, with or without the neutralizing CCL5 Ab. Each symbol represents an individual measurement, and the horizontal bar represents the mean. **(H)** Immunosuppressive activity of MDSCs on stimulated autologous T-cell proliferation. T-cell activation was induced by anti-CD3/CD28-coated beads and IL-2. *$P < 0.05$; **$P < 0.01$.

cell proliferation and IFNγ production *in vitro* associated with high levels of iNOS expression, whereas that of KO mice expressed lower levels of NO and displayed diminished immunosuppressive activity. The PMN subset from both WT and KO mice exhibited much lower immunosuppressive activity and NO production *in vitro*, consistent with a recent report [18].

In addition to L-arginine depletion through ARG1-dependent consumption and generation of ROS produced by ARG1 and iNOS, the mechanism of MDSCs whereby to influence the immune response also involves activation and expansion of Treg cell populations [40]. In mouse models, studies have shown that MDSCs induce the conversion of naïve CD4^{+} T cells into induced Treg cells [41, 42]. At the same time, clinic data have demonstrated that human CD14^{+} HLA^{-} DR^{low/-} MDSCs produce TGF-β and retinoic acid, which can convert Th17 cells into Treg cells [43]. A new study also found that tumor-derived CCL5/CCR5 signaling helps recruit Tregs to tumors and enhances Tregs' ability to kill antitumor CD8^{+} T cell by producing TGF-β [44].

Although the major functions of chemokines are manifested in activities in attracting and activating leukocytes at sites of inflammation and injury, some studies have found that chemokines also have regulatory effects on the proliferation of myeloid progenitor cells [45]. Macrophage inflammatory (MIP)-1α (also CCL3) is the most studied, and it has suppressive effects on the proliferation of early subsets of hematopoietic stem cells and progenitors [45, 46]. However, by staining bone marrow cells for CD34 and FcγR expression (data not shown), we showed that CCL5 does not affect GMP (granulocyte/macrophage progenitor), and suggest that CCL5 plays a major role in the macrophage and neutrophil cell fate specification.

Hematopoietic cell fate specification depends on induction as well as repression of subsets of lineage-specific genes, and hematopoietic transcription factors are essential for it. The relative level of PU.1 and C/EBPα in granulocyte/macrophage progenitors has been proved to regulate the choice between macrophage and neutrophil cell fate specification [47]. Recently one group described a new gene regulatory network underlying macrophage and neutrophil cell fates, showing that PU.1 modulates a novel regulatory circuit comprised of counter antagonistic repressors, Egr-1, 2/Nab-2 and Gfi-1 [48]. How does CCL5 regulate this complicated network? Another study may have yielded some clues as it showed that cytokines could promote cell fate decision by altering the relative concentration of lineage-determining transcriptional regulators [47].

Our analyses showed that in the bone marrow of tumor-bearing KO mice, the population of granulocytes had higher Ly6C expression, almost merging with the MO subset. These Ly6C^{hi} and Ly6G^{+} cells are distinct from the Ly6C and Ly6G-double positive granulocytes described recently [28]. In addition to changes in myeloid cells, there were higher frequencies in the more mature population of blasts and progenitors in KO mice.

Previous studies by others have mostly focused on tumor-derived CCL5, and found overexpression of CCL5 in advanced stages of breast cancer [5]. In more recent years, mesenchymal stem cell-derived CCL5 has been shown to contribute to cancer cell motility, invasion and metastasis [49, 50]. 4T1 growth characteristics parallel highly invasive human metastatic mammary carcinoma comparable with human stage IV breast cancer [51]. 4T1 tumors, being ER-α-, PR- and HER-2/neu-negative, resembling human "triple negative" breast cancer, which is a highly aggressive malignancy lacking a historical therapeutic target. In this model, we did not observe the upregulation of CCL5 expression in tumor cells. Furthermore, we showed that tumor-derived CCL5 has no effect on tumor growth, consistent with findings by a previous study [15]. In contrast, our data demonstrate for the first time a novel and critical role of hematopoietic CCL5 in the development of MDSCs.

Since immune suppression plays a crucial role in promoting tumor progression and failure of cancer vaccines, among which MDSCs are the major immunosuppressive effectors, different strategies have been used to overcome MDSC-mediated immunosuppression. Our study suggests that targeting CCL5 in breast cancer can decrease the immunosuppression activity of MDSCs, improve vaccine efficacy against poorly immunogenic tumors, and reduce breast cancer progression and metastasis. Targeting CCL5 is feasible because it is apparently dispensable in development and physiology with no apparent immunodeficiency, due perhaps to redundancies. Targeted inhibition of CCL5 to the hematopoietic compartment in select breast cancer patients, particularly the triple-negative type, may have strong therapeutic impact without overt toxicity.

Materials and Methods

Mice

WT BALB/c mice were purchased from the Jackson Laboratories (Bar Harbor, ME, USA). CCL5 KO mice were generously provided by Dr S Sarawar (Torrey Pines Institute for Molecular Studies, San Diego, CA, USA) after >10 generations of back-crossing to BALB/c from the original C57BL/6 background [52]. CCL5 KO mice have no morphologically or functionally overt abnormal phenotype. CL4 mice are transgenic for the K[d]-restricted HA[512-520] peptide-specific TCR in a BALB/c background (Jackson Labora-

tories). Transgenic mice expressing Wnt-1 have been described [53]. Genotyping was done using PCR of tail DNAs. The mice are in the FVB background and usually develop mammary tumors between the age of 2 and 8 months. Tumors were collected when they reached the size of 1.5 to 2.0 cm in diameter. Some of the tumors used in this study were from mice orthotopically transplanted with the primary tumors.

Administration of anti-CCL5 in vivo

The *in vivo* effective neutralizing antibody against murine CCL5 mAb was obtained from Dr Thomas Lane (University California, Irvine, USA) An irrelevant isotype-matched IgG was used as the control. 4T1 tumor-bearing WT mice (five per group) were treated via i.p. injection with 100 µg of either anti-CCL5 or control IgG suspended in 500 µl of sterile PBS on days 7 and 14 post tumor injection. For therapeutic vaccine model, tumor-bearing mice (five per group) were injected with anti-CCL5 or control IgG, followed by i.p. injection of 2×10^6 irradiated (12 000 rad) 4T1 cells on days 0, 3, and 7.

Cell sorting

To purify MDSCs (CD11b$^+$, Gr-1$^+$), splenocytes were first negatively selected by anti-CD19 and anti-CD11c microbeads and LD columns to eliminate CD11b$^+$, Gr-1$^-$ cells. The remaining cells were positively selected by anti-CD11b microbeads and LS column to obtain pure MDSC cells. To purify PMN and MO-MDSC subsets, 1×10^8 erythrocyte-depleted splenocytes were firstly blocked with FcγR and stained with anti-Ly6G-biotin, followed by positive magnetic selection with anti-biotin-microbeads, according to the manufacturer's suggested protocols. The negative fraction from previous step was passed over an LD depletion column to eliminate the remaining Ly6G$^+$ cells. To further purify the MO-MDSCs, remaining cells were sequentially stained with anti-Ly6G-biotin and streptavidin microbeads; the MO-MDSC subset was sorted with LS column. All microbeads and columns were from Miltenyi Biotec.

Immune function assay

CD8$^+$ T cells from CL4 mice transgenic for HA$_{512-520}$-specific TCR were used as responder cells. Purified MDSC subsets were added to 1×10^6 CL4 splenocytes in different ratios in the presence of 1 µg/ml of HA$_{512-520}$. 48 h later, 10 mM ErdU was added to the culture and cells were allowed to proliferate for another 18 h before harvest and analyzed by flow cytometry.

MDSC adoptive transfer

3×10^6 MDSCs isolated from spleens of WT and CCL5 KO mice bearing 4T1 tumors were injected i.v. into either WT or KO recipient mice. Adoptive transfer of MDSCs to recipient mice was performed 4 days after inoculation with 4T1 cells, and then given every 7 days thereafter for 3 weeks. Tumors at the site of injection were measured using an electronic calipers and tumor diameters were calculated as the square root of the length × width of the tumor as previously described [16, 54]. Mice were sacrificed for endpoint analyses when the diameter of the tumor reached > 20 mm.

ELISPOT assay

MDSC subsets were isolated from spleens of tumor-bearing mice. Splenocytes from CL4 mice were used as responder cells. 5 $\times 10^4$ MDSCs and 2×10^5 responder cells were incubated at 37 °C

for 24 h. The number of IFNγ-positive spots in response to the specific peptide was measured by ELISPOT according to the manufacturer's suggested procedure (eBioscience). For ELISPOT assay of T cells from tumor-bearing mice, spleens from tumor-bearing mice inoculated with 4T1 cells 2 weeks earlier were used as responder cells. 2×10^5 responder cells were cultured with 2×10^4 irradiated (100 Gy) 4T1 cells at 37 °C for 48 h.

Bone marrow transplantation

2×10^7 bone marrow cells from male donor WT or KO mice were injected via the tail vein into recipient female WT and KO mice lethally irradiated 24 h prior to 8.5 Gy of radiation. After 30 days, the efficiency of chimera establishment was assessed by PCR analysis of DNA from PBMCs for X and Y chromosomes. The primers and PCR conditions were described previously [55].

Colony formation assays

Colony formation assays were done as described previously [56]. Single-cell suspensions of bone marrow (2.5×10^4 cells/ml) from WT and KO mice were plated in 1 ml methylcellulose medium (MethoCult GF M3231, StemCell Technologies) with different doses of G-CSF, M-CSF or GM-CSF and incubated at 37 °C and 5% CO_2 for 12 days.

Human MDSCs

As previously described [32], PBMCs from healthy donors were isolated by differential density gradient separation. PBMC were cultured in complete medium with GM-CSF (10 ng/ml) and IL-6 (10 ng/ml) for 7 days. MDSCs were analyzed by flow cytometry after labeling and characterized by the CD33$^+$ HLA-DR$^-$ CD3$^-$ phenotype. MDSCs were isolated from the PBMC cultures using anti-CD33 magnetic microbeads (Miltenyi Biotec), following manufacturer's instruction. Some cells were treated with 10 µg/ml anti-GM-CSF antibody and 15 µg/ml anti-CCL5 antibody (R&D systems). The immunosuppressive activity of MDSCs was evaluated by their ability to inhibit the proliferation of autologous T cells. T cells were purified from PBMC of autologous donors using CD3$^+$ T-cell enrichment column (R&D Systems), following manufacturer's instruction. T cells were added to isolated MDSCs in a 2:1 ratio, and stimulated by anti-CD3/CD28 stimulation beads (Invitrogen) and IL-2 (100 u/ml). Two days later, 10 mM ErdU was added to the culture and cells were allowed to proliferate for another 24 h before harvest and analyzed by flow cytometry.

Statistical analysis

Mann-Whitney test was used to analyze the data. Results are given as mean ± SD unless otherwise indicated. Probability values < 0.05 were considered statistically significant.

Acknowledgments

References

1   Appay V, Rowland-Jones SL. RANTES: a versatile and controversial chemokine. *Trends Immunol* 2001; **22**:83-87.

2 Levy JA. The unexpected pleiotropic activities of RANTES. *J Immunol* 2009; **182**:3945-3946.

3 Pakianathan DR, Kuta EG, Artis DR, Skelton NJ, Hebert CA. Distinct but overlapping epitopes for the interaction of a CC-chemokine with CCR1, CCR3 and CCR5. *Biochemistry* 1997; **36**:9642-9648.

4 Movahedi K, Guilliams M, Van den Bossche J, *et al.* Identification of discrete tumor-induced myeloid-derived suppressor cell subpopulations with distinct T cell-suppressive activity. *Blood* 2008; **111**:4233-4244.

5 Yaal-Hahoshen N, Shina S, Leider-Trejo L, *et al.* The chemokine CCL5 as a potential prognostic factor predicting disease progression in stage II breast cancer patients. *Clin Cancer Res* 2006; **12**:4474-4480.

6 Niwa Y, Akamatsu H, Niwa H, Sumi H, Ozaki Y, Abe A. Correlation of tissue and plasma RANTES levels with disease course in patients with breast or cervical cancer. *Clin Cancer Res* 2001; **7**:285-289.

7 Nouh MA, Eissa SA, Zaki SA, El-Maghraby SM, Kadry DY. Importance of Serum IL-18 and RANTES as Markers for Breast Carcinoma Progression. *J Egypt Natl Canc Inst* 2005; **17**:51-55.

8 Bieche I, Lerebours F, Tozlu S, Espie M, Marty M, Lidereau R. Molecular profiling of inflammatory breast cancer: identification of a poor-prognosis gene expression signature. *Clin Cancer Res* 2004; **10**:6789-6795.

9 Wigler N, Shina S, Kaplan O, *et al.* Breast carcinoma: a report on the potential usage of the CC chemokine RANTES as a marker for a progressive disease. *Isr Med Assoc J* 2002; **4**:940-943.

10 Sauer G, Schneiderhan-Marra N, Kazmaier C, *et al.* Prediction of nodal involvement in breast cancer based on multiparametric protein analyses from preoperative core needle biopsies of the primary lesion. *Clin Cancer Res* 2008; **14**:3345-3353.

11 Luboshits G, Shina S, Kaplan O, *et al.* Elevated expression of the CC chemokine regulated on activation, normal T cell expressed and secreted (RANTES) in advanced breast carcinoma. *Cancer Res* 1999; **59**:4681-4687.

12 Adler EP, Lemken CA, Katchen NS, Kurt RA. A dual role for tumor-derived chemokine RANTES (CCL5). *Immunol Lett* 2003; **90**:187-194.

13 Robinson SC, Scott KA, Wilson JL, Thompson RG, Proudfoot AE, Balkwill FR. A chemokine receptor antagonist inhibits experimental breast tumor growth. *Cancer Res* 2003; **63**:8360-8365.

14 Soria G, Ben-Baruch A. The inflammatory chemokines CCL2 and CCL5 in breast cancer. *Cancer Lett* 2008; **267**:271-285.

15 Jayasinghe MM, Golden JM, Nair P, O'Donnell CM, Werner MT, Kurt RA. Tumor-derived CCL5 does not contribute to breast cancer progression. *Breast Cancer Res Treat* 2008; **111**:511-521.

16 Ostrand-Rosenberg S, Grusby MJ, Clements VK. Cutting edge: STAT6-deficient mice have enhanced tumor immunity to primary and metastatic mammary carcinoma. *J Immunol* 2000; **165**:6015-6019.

17 Kelner GS, Kennedy J, Bacon KB, *et al.* Lymphotactin: a cytokine that represents a new class of chemokine. *Science* 1994; **266**:1395-1399.

18 Dolcetti L, Peranzoni E, Ugel S, *et al.* Hierarchy of immunosuppressive strength among myeloid-derived suppressor cell subsets is determined by GM-CSF. *Eur J Immunol* 2010; **40**:22-35.

19 Sawanobori Y, Ueha S, Kurachi M, *et al.* Chemokine-mediated rapid turnover of myeloid-derived suppressor cells in tumor-bearing mice. *Blood* 2008; **111**:5457-5466.

20 Youn JI, Nagaraj S, Collazo M, Gabrilovich DI. Subsets of myeloid-derived suppressor cells in tumor-bearing mice. *J Immunol* 2008; **181**:5791-5802.

21 Zhu B, Bando Y, Xiao S, *et al.* CD11b+Ly-6C(hi) suppressive monocytes in experimental autoimmune encephalomyelitis. *J Immunol* 2007; **179**:5228-5237.

22 Melani C, Chiodoni C, Forni G, Colombo MP. Myeloid cell expansion elicited by the progression of spontaneous mammary carcinomas in c-erbB-2 transgenic BALB/c mice suppresses immune reactivity. *Blood* 2003; **102**:2138-2145.

23 Ling V, Luxenberg D, Wang J, *et al.* Structural identification of the hematopoietic progenitor antigen ER-MP12 as the vascular endothelial adhesion molecule PECAM-1 (CD31). *Eur J Immunol* 1997; **27**:509-514.

24 Gabrilovich DI, Nagaraj S. Myeloid-derived suppressor cells as regulators of the immune system. *Nat Rev Immunol* 2009; **9**:162-174.

25 Katz BZ, Eshel R, Sagi-Assif O, Witz IP. An association between high Ly-6A/E expression on tumor cells and a highly malignant phenotype. *Int J Cancer* 1994; **59**:684-691.

26 Trottier MD, Newsted MM, King LE, Fraker PJ. Natural glucocorticoids induce expansion of all developmental stages of murine bone marrow granulocytes without inhibiting function. *Proc Natl Acad Sci USA* 2008; **105**:2028-2033.

27 de Bruijn MF, Slieker WA, van der Loo JC, Voerman JS, van Ewijk W, Leenen PJ. Distinct mouse bone marrow macrophage precursors identified by differential expression of ER-MP12 and ER-MP20 antigens. *Eur J Immunol* 1994; **24**:2279-2284.

28 Shojaei F, Wu X, Qu X, *et al.* G-CSF-initiated myeloid cell mobilization and angiogenesis mediate tumor refractoriness to anti-VEGF therapy in mouse models. *Proc Natl Acad Sci USA* 2009; **106**:6742-6747.

29 Shojaei F, Wu X, Zhong C, *et al.* Bv8 regulates myeloid-cell-dependent tumour angiogenesis. *Nature* 2007; **450**:825-831.

30 Kusmartsev S, Cheng F, Yu B, *et al.* All-trans-retinoic acid eliminates immature myeloid cells from tumor-bearing mice and improves the effect of vaccination. *Cancer Res* 2003; **63**:4441-4449.

31 Li Y, Hively WP, Varmus HE. Use of MMTV-Wnt-1 transgenic mice for studying the genetic basis of breast cancer. *Oncogene* 2000; **19**:1002-1009.

32 Lechner MG, Liebertz DJ, Epstein AL. Characterization of cytokine-induced myeloid-derived suppressor cells from normal human peripheral blood mononuclear cells. *J Immunol* 2010; **185**:2273-2284.

33 Seung LP, Rowley DA, Dubey P, Schreiber H. Synergy between T-cell immunity and inhibition of paracrine stimulation causes tumor rejection. *Proc Natl Acad Sci USA* 1995; **92**:6254-6258.

34 Bronte V, Chappell DB, Apolloni E, *et al.* Unopposed production of granulocyte-macrophage colony-stimulating factor by

tumors inhibits CD8+ T cell responses by dysregulating antigen-presenting cell maturation. *J Immunol* 1999; **162**:5728-5737.

35 Salvadori S, Martinelli G, Zier K. Resection of solid tumors reverses T cell defects and restores protective immunity. *J Immunol* 2000; **164**:2214-2220.

36 Terabe M, Matsui S, Park JM, *et al.* Transforming growth factor-beta production and myeloid cells are an effector mechanism through which CD1d-restricted T cells block cytotoxic T lymphocyte-mediated tumor immunosurveillance: abrogation prevents tumor recurrence. *J Exp Med* 2003; **198**:1741-1752.

37 Danna EA, Sinha P, Gilbert M, Clements VK, Pulaski BA, Ostrand-Rosenberg S. Surgical removal of primary tumor reverses tumor-induced immunosuppression despite the presence of metastatic disease. *Cancer Res* 2004; **64**:2205-2211.

38 Serafini P, Borrello I, Bronte V. Myeloid suppressor cells in cancer: recruitment, phenotype, properties, and mechanisms of immune suppression. *Semin Cancer Biol* 2006; **16**:53-65.

39 Hock H, Hamblen MJ, Rooke HM, *et al.* Intrinsic requirement for zinc finger transcription factor Gfi-1 in neutrophil differentiation. *Immunity* 2003; **18**:109-120.

40 Gabrilovich DI, Ostrand-Rosenberg S, Bronte V. Coordinated regulation of myeloid cells by tumours. *Nat Rev Immunol* 2012; **12**:253-268.

41 Pan PY, Ma G, Weber KJ, *et al.* Immune stimulatory receptor CD40 is required for T-cell suppression and T regulatory cell activation mediated by myeloid-derived suppressor cells in cancer. *Cancer Res* 2010; **70**:99-108.

42 Serafini P, Mgebroff S, Noonan K, Borrello I. Myeloid-derived suppressor cells promote cross-tolerance in B-cell lymphoma by expanding regulatory T cells. *Cancer Res* 2008; **68**:5439-5449.

43 Hoechst B, Gamrekelashvili J, Manns MP, Greten TF, Korangy F. Plasticity of human Th17 cells and iTregs is orchestrated by different subsets of myeloid cells. *Blood* 2011; **117**:6532-6541.

44 Chang LY, Lin YC, Mahalingam J, *et al.* Tumor-derived chemokine CCL5 enhances TGF-beta-mediated killing of CD8(+) T cells in colon cancer by T-regulatory cells. *Cancer Res* 2012; **72**:1092-1102.

45 Broxmeyer HE, Sherry B, Lu L, *et al.* Enhancing and suppressing effects of recombinant murine macrophage inflammatory proteins on colony formation in vitro by bone marrow myeloid progenitor cells. *Blood* 1990; **76**:1110-1116.

46 Broxmeyer HE, Sherry B, Cooper S, *et al.* Macrophage inflammatory protein (MIP)-1 beta abrogates the capacity of MIP-1 alpha to suppress myeloid progenitor cell growth. *J Immunol* 1991; **147**:2586-2594.

47 Dahl R, Walsh JC, Lancki D, *et al.* Regulation of macrophage and neutrophil cell fates by the PU.1:C/EBPalpha ratio and granulocyte colony-stimulating factor. *Nat Immunol* 2003; **4**:1029-1036.

48 Laslo P, Spooner CJ, Warmflash A, *et al.* Multilineage transcriptional priming and determination of alternate hematopoietic cell fates. *Cell* 2006; **126**:755-766.

49 Karnoub AE, Dash AB, Vo AP, *et al.* Mesenchymal stem cells within tumour stroma promote breast cancer metastasis. *Nature* 2007; **449**:557-563.

50 Mi Z, Bhattacharya SD, Kim VM, Guo H, Talbot LJ, Kuo PC. Osteopontin promotes CCL5-mesenchymal stromal cell-mediated breast cancer metastasis. *Carcinogenesis* 2011; **32**:477-487.

51 Guy CT, Cardiff RD, Muller WJ. Induction of mammary tumors by expression of polyomavirus middle T oncogene: a transgenic mouse model for metastatic disease. *Mol Cell Biol* 1992; **12**:954-961.

52 Wareing MD, Lyon AB, Lu B, Gerard C, Sarawar SR. Chemokine expression during the development and resolution of a pulmonary leukocyte response to influenza A virus infection in mice. *J Leukoc Biol* 2004; **76**:886-895.

53 Tsukamoto AS, Grosschedl R, Guzman RC, Parslow T, Varmus HE. Expression of the int-1 gene in transgenic mice is associated with mammary gland hyperplasia and adenocarcinomas in male and female mice. *Cell* 1988; **55**:619-625.

54 Poh TW, Bradley JM, Mukherjee P, Gendler SJ. Lack of Muc1-regulated beta-catenin stability results in aberrant expansion of CD11b+Gr1+ myeloid-derived suppressor cells from the bone marrow. *Cancer Res* 2009; **69**:3554-3562.

55 Novak EK, Reddington M, Zhen L, *et al.* Inherited thrombocytopenia caused by reduced platelet production in mice with the gunmetal pigment gene mutation. *Blood* 1995; **85**:1781-1789.

56 Karsunky H, Zeng H, Schmidt T, *et al.* Inflammatory reactions and severe neutropenia in mice lacking the transcriptional repressor Gfi1. *Nat Genet* 2002; **30**:295-300.

(**Supplementary information** is linked to the online version of the paper on the *Cell Research* website.)